

Abstract number 596

# Inclusive Lifetime and Mixing Measurements Using Topological Vertexing

The ALEPH Collaboration

OPEN-99-333  
19/08/1997



## Abstract

Measurements of the inclusive  $b$ -hadron lifetime and  $B_d^0 - \overline{B}_d^0$  time-dependent mixing are presented. Events are selected and tagged using topological vertexing techniques. Proper-time reconstruction is performed by revertexing with a vertex-charge weighting algorithm to reconstruct the  $b$ -hadron momentum. Systematic studies are made of the  $b$ -hadron momentum reconstruction, proper time resolution, Monte Carlo reweighting and corrections used in the fitting procedure. Making use of the full LEP 1 dataset yields a preliminary inclusive  $b$  lifetime of :  $\tau_b = 1.601 \pm 0.004$  (stat.)  $\pm 0.032$  (syst.)  $ps$ . A fit is performed to the product of the charges in opposite  $b\overline{b}$  hemispheres, using a double jet-charge method to determine the combination of initial and final states. This yields a competitive measurement of the  $B_d^0 - \overline{B}_d^0$  mixing parameter :  $\Delta m_d = 0.441 \pm 0.026$  (stat.)  $\pm 0.029$  (syst.)  $ps^{-1}$ .

Contribution to EPS-HEP Conference, Jerusalem, August 1997

# 1 Introduction

Measurements of the inclusive  $b$  hadron lifetime and the  $B_d^0 - \overline{B}_d^0$  mixing parameter are presented, using a sample of approximately four million hadronic  $Z^0$  decays collected with the ALEPH detector at LEP.

An inclusive double hemisphere tagging technique is used in order to maximise the statistical precision of the measurements. The method benefits from having approximately five times the statistics of other measurements. Events are  $b$ -tagged, and decay lengths reconstructed, using inclusive vertexing techniques. A smearing procedure is applied to tracks in the Monte Carlo simulation in order to improve the agreement with data and hence control systematic uncertainties. A weighting procedure is used in reconstructing the charged  $b$  hadron momentum before adding neutral and missing energy components using calorimetric information. These are combined with the decay length information to give a typical proper time resolution estimated to be 0.23 ps.

The  $b$  hadron lifetime fitting procedure incorporates the effects of proper time resolution by means of folding matrices, and takes into account the vertexing efficiencies as a function of proper time, using comparisons with data as far as possible to estimate systematic uncertainties.

A jet-charge method is used to determine the states of  $B$  mesons at production and decay, based on the fact that the jet-charge for mesons which have undergone mixing is different from that for unmixed mesons. A multi-parameter fit is performed to the product of the jet-charges in the two event hemispheres, plotted as a function of reconstructed proper time. This gives a measurement of the  $B_d$  oscillation frequency.

## 2 Event Selection and $b$ -Tagging

Hadronic events are selected from a total of approximately 4.1 million events collected between 1991 and 1995. Events are selected to have at least 5 tracks satisfying the criterion : to originate from a cylinder of radius 2 cm and length 20 cm around the interaction point, have at least four time-projection chamber hits and have  $|\cos\theta| < 0.95$ , where  $\theta$  is the angle of the track with respect to the beam axis. The total energy of all 'good' charged tracks must be more than 10% of the centre-of-mass energy.

For events which pass these basic selection cuts, the thrust axis is calculated. Events with  $|\cos\theta_{thrust}| < 0.8$  are accepted and the others are discarded. This is essential for secondary vertex reconstruction. Each event is then separated into two hemispheres using the plane perpendicular to the thrust axis.

Secondary vertices are reconstructed using an inclusive pattern recognition package which is based on a search in coordinate space rather than a search amongst track combinations. Prior to using this algorithm, jet-finding is performed on all energy flow objects, using the JADE algorithm with a  $y_{cut}$  of 0.02. Two jets are chosen as being those most likely to contain the  $b$  hadron decay vertices; the most energetic jet and the one which forms the highest invariant mass with it. The small fraction of events ( $\sim 0.06\%$ ) in which the two chosen jets are in the same hemisphere are rejected. A quantity called  $\Delta\chi^2$  is defined as the difference between the  $\chi^2$  when all tracks are assigned to the primary vertex, and the sum of the primary and secondary vertex  $\chi^2$  values when some tracks are assigned to a possible secondary. The value of  $\Delta\chi^2$  is calculated for various secondary vertex positions on a grid extending  $\pm 1$  cm along the jet direction and  $\pm 500 \mu\text{m}$  in the orthogonal direction. The point of maximum  $\Delta\chi^2$  is chosen as the secondary vertex position. This procedure is carried out for both jets therefore giving a secondary vertex position for each hemisphere. As long as there are usable tracks in the hemisphere a secondary vertex is always found.

The significance of the vertex can be estimated by the size of  $\Delta\chi^2$ . Large values of  $\Delta\chi^2$  can therefore be used to tag  $b$  decays by requiring that it is large. An event tag is used, based on a cut on the sum of the  $\Delta\chi^2$  variables in both hemispheres. The quantity  $\sum_{hemispheres} (\Delta\chi^2) / 2$  is referred to as the BTAG. Using a BTAG cut on the event as a whole has the advantage of being much more efficient, whilst the bias introduced is taken into account in the fitting procedure.

## 3 Measurement of Decay Length

A two stage process is used to calculate the decay length of the  $b$  hadron. The initial primary and secondary vertex position found in each hemisphere using the topological vertex finder allows the quantity, denoted by  $\mathcal{R}_{sig}$ , to be defined for each track :

$$\mathcal{R}_{sig} = \frac{\mathcal{S}_p}{\mathcal{S}_p + \mathcal{S}_s} \quad (1)$$

The quantities  $\mathcal{S}_p$  and  $\mathcal{S}_s$  are the track significances<sup>1</sup> relative to the primary and secondary vertices respectively. The quantities  $\mathcal{S}_p$  and  $\mathcal{S}_s$  are signed relative to the jet-axis. The quantity  $\mathcal{R}_{sig}$  provides a means of distinguishing between fragmentation tracks and those from the  $b$ -hadron decay. Most fragmentation tracks have  $\mathcal{R}_{sig}$  smaller than  $\sim 0.5$  while  $b$ -hadron tracks tend to have higher values of  $\mathcal{R}_{sig}$ .

The decay length resolution is significantly improved by choosing the subset of tracks which have  $\mathcal{R}_{sig} > 0.7$  and fitting them to form a new secondary vertex. The decay length is then given by the distance between the primary vertex and this revertexed secondary, signed relative to the jet direction. From Monte Carlo  $b$  events it is determined that about 80% of tracks assigned to the secondary vertex by an  $\mathcal{R}_{sig}$  cut of 0.7 are  $b$ -hadron tracks and the remaining 20% are fragmentation tracks.

If both hemispheres contain secondary vertices with a  $\chi^2$  probability of greater than 1%, then the hemisphere containing the vertex with the highest  $\chi^2$  probability is chosen to be the side on which the proper time is measured and if there is only one good secondary vertex then that hemisphere is chosen. Events in which neither hemisphere contains a good secondary vertex are rejected. The resulting decay length reconstruction efficiency for hemispheres is approximately 85% on average and about 93% for  $b$  events.

The decay length resolution from revertexing in this way is estimated in Monte Carlo to have a Gaussian width of 0.24mm for 75% of events and 0.64mm for 22% of events.

## 4 Measurement of the $b$ -hadron Momentum

The momentum of the  $b$ -hadron is composed of three contributions :

- Charged tracks from the  $b$ -hadron decay, which contribute, on average, 60% of the total  $b$ -hadron momentum.
- Neutral particles from the  $b$  decay, which constitute around 34% of the total  $b$ -hadron momentum. These are particles such as  $\gamma$  and  $\pi^0$  which are detected in the ECAL and particles such as neutrons which are detected in HCAL.
- The third contribution comes from missing momentum which is carried by undetected neutrinos which may be produced in the  $b$  decay, contributing 6% on average.

In order to reconstruct the momentum contribution from charged tracks it is again necessary to distinguish between  $b$ -hadron decay tracks and fragmentation tracks. This is done using the rapidity of tracks relative to the secondary vertex direction.

The charged contribution to the  $b$ -hadron momentum is found by summing the momenta of all charged tracks in the hemisphere, weighted by the probability that they are from the  $b$ -hadron decay :

$$p_B^{ch} = \sum_{i = \text{charged tracks}} w_i p_i \quad (2)$$

where  $w_i$  is the weight assigned to track  $i$  and  $p_i$  is the track momentum.

Assigning neutral energy to the  $b$ -hadron decay is slightly more difficult than calculating the contribution due to charged tracks. The procedure is as follows :

- Jet clustering is performed on all neutral and charged objects, using the JADE algorithm with a  $y_{cut}$  corresponding to the average mass of the  $b$ -hadron.
- The jet which is closest to the secondary vertex direction is chosen to be the  $b$ -hadron jet.
- If a neutral object is in the chosen jet, then its momentum component parallel to the vertex direction is included in the total  $b$ -hadron momentum.

The missing energy due to undetected neutrinos is calculated by subtracting the visible energy in the hemisphere from the total energy in that hemisphere :

$$E_{hemi i}^{miss} = E_{hemi i}^{tot} - E_{hemi i}^{vis} \quad (3)$$

where the total energy in hemisphere 1,  $E_{hemi 1}^{tot}$  is calculated using conservation of energy and momentum :

$$E_{hemi 1}^{tot} = \frac{\sqrt{s}}{2} + \frac{m_{hemi 1}^2 - m_{hemi 2}^2}{2\sqrt{s}} \quad (4)$$

---

<sup>1</sup>The track *significance* is the signed impact parameter (relative to the primary or secondary vertex) divided by its error.

and  $m_{hemi\ 1,2}$  are the invariant masses of the two hemispheres. In order to estimate the missing energy resolution, the negative side of the missing energy distributions in data and Monte Carlo are fitted with Gaussians. Only the fraction of missing energy which lies outside of the fitted resolution envelope is used.

The momentum resolution is approximately 9% for 80% of events on average and is a strong function of  $p_{true}$ .

## 5 Proper Time Resolution

The reconstructed proper time distribution which is obtained using the decay length and momentum algorithms described above are in good agreement between data and Monte Carlo simulation. The agreement is also good in the negative tail indicating that the proper time resolution is well modelled in the Monte Carlo after additional track smearing has been performed.

The average proper time resolution is given as the results of a triple Gaussian fit given in Table 1. The core

Parameter	Gaussian 1	Gaussian 2	Gaussian 3
Amplitude	75%	22%	3%
Mean (ps)	0.027	0.0002	-0.17
$\sigma$ (ps)	0.23	0.65	2.1

Table 1: *Results of a triple Gaussian fit to the average proper time resolution.*

75% of events have a resolution of about 0.23 ps.

## 6 Outline of the Fitting Procedure for the $b$ -hadron Lifetime

The lifetime fitting procedure consists of a MINUIT minimisation of the  $\chi^2$  difference between the reconstructed proper time distribution in data and a “theoretical” distribution which is constructed by folding detector resolution effects with a true  $b$  lifetime distribution and adding background components. The basic structure of the lifetime fit is as follows :

- (a) Begin with the true  $b$  proper time distribution,  $e^{-\frac{t}{\tau_b}}$ .
- (b) Modify the true  $b$  distribution by the time dependent vertexing efficiency  $\epsilon^{vtx}(t)$  which is taken from Monte Carlo.
- (c) Incorporate proper time resolution effects by folding the time distribution with the resolution matrix which is derived from Monte Carlo. This gives a “reconstructed”  $b$  proper time distribution, prior to the effects of the  $b$  tagging.
- (d) Modify this reconstructed distribution by the time dependent  $b$  tagging efficiency to obtain a final reconstructed distribution for  $b$ -hadrons.
- (e) Add the contributions from  $c$  and  $uds$  backgrounds to obtain a “theoretical” proper time distribution which is then fitted to data by varying the lifetime,  $\tau_b$ , in the true  $b$  proper time distribution.

The fitted purities are determined to be :

$$\mathcal{P}_b = (87.2 \pm 1.2)\% \text{ (89.3\% expected)}, \quad \mathcal{P}_c = (9.7 \pm 1.8)\% \text{ (7.3\% expected)}$$

## 7 Results and Contributions to the error on $\tau_b$

A summary of contributions to the systematic uncertainty on the inclusive  $b$ -hadron lifetime are given in Table 2. These systematic uncertainties are determined from the following considerations :

- **Monte Carlo Statistics** : Errors associated with the resolution folding matrix and the shape of the reconstructed proper time distributions for  $c$  and  $uds$  events are incorporated in the fit procedure.
- **Efficiency Corrections** : The error due to the  $b$  tagging efficiency corrections is calculated using the difference between data and Monte Carlo bin-by-bin efficiencies as a function of reconstructed proper time.

<i>Source of Uncertainty</i>	$\sigma_{\tau_b}$ (ps)
<i>Monte Carlo statistics</i>	$\pm 0.002$
<i>BTAG Efficiency corrections</i>	$\pm 0.013$
<i>Sample Flavour composition</i>	$\pm 0.006$
<i>Primary heavy flavour fractions and lifetimes</i>	$\pm 0.001$
<i>Secondary charm decay fractions and lifetimes</i>	$\pm 0.015$
<i>b fragmentation</i>	$\pm 0.024$
Total	$\pm 0.032$

Table 2: *Summary of the various contributions to the systematic error on  $\tau_b$ .*

- **Flavour Composition :** The systematic error due to the flavour composition is determined by fixing the  $b$  and  $c$  purities and subtracting the resulting error on  $\tau_b$  in quadrature from the error obtained when the purities are allowed to vary within constraints. The constraints are determined from the data-Monte Carlo agreement in the overall single and double-tag hemisphere efficiencies.
- **Primary & Secondary Heavy Flavour Fractions and Lifetimes :** Branching fractions, decay modes and lifetimes are reweighted in the Monte Carlo simulation. In the case of charm decays, this is done for both primary and secondary charm production. For  $b$  hadron decays, the most up-to-date lifetimes and branching fractions are used in determining the corrections used in the fit. The systematic uncertainty is determined as the difference in the fitted lifetimes when using the most up-to-date values as compared to their Monte Carlo defaults.
- **$b$  Fragmentation :** The error due to the knowledge of the  $b$  fragmentation function is estimated by reweighting the Monte Carlo using different values of the Peterson fragmentation parameter,  $\epsilon_b$ . Variations of  $\pm 0.0014$  are used about a central value of 0.0045.

Performing the fit on the combined 1991 to 1995 data set, using the combined Monte Carlo sample gives the lifetime result :

$$\tau_b = 1.601 \pm 0.004 (\text{stat.}) \pm 0.032 (\text{syst.}) \text{ ps}$$

The result of the fit is shown in Figure 1. The  $\chi^2/\text{n.d.f}$  is 42/49 and relatively low since the errors include both contributions from statistics and from systematic errors arising from the  $b$  tagging efficiency corrections.

## 8 Time-Dependent Mixing Analysis

The analysis of rates of  $B_d^0 - \overline{B}_d^0$  and  $B_s^0 - \overline{B}_s^0$  oscillations can be considered as an extension of the inclusive  $b$  lifetime measurement. The method used here utilises the so-called jet-charge information in both hemispheres of tagged events as a means of tagging both initial and final state quark charges. This gives a continuous variable, between 0 and 1, which supplies charge information about both the initial and final states. As a consequence of the continuous nature of the jet-charge measurement, what is observed in the mixing analysis is a time-dependent reduction of the jet-charge product between the hemisphere in which the proper decay time is measured and the opposite hemisphere. The rate in proper time with which the effective mistag is degraded, depends on the values of  $\Delta m_d$  and  $\Delta m_s$ .

### 8.1 The Charge Correlation Function

The charge correlation function for data is defined as the product of the two hemisphere charges :

$$\text{charge correlation} = \langle -Q_{jo}^{\kappa=0.5} Q_{js}^{\kappa=1.0} \rangle (t) \quad (5)$$

where ‘s’ refers to the “same” hemisphere in which the proper time is measured and ‘o’ refers to the “opposite” hemisphere. The jet-charge in the opposite hemisphere reflects, on average, the initial quark charge in that hemisphere and hence gives information on the initial charge in the “same” hemisphere since initially a  $b\overline{b}$  pair are produced. The choice of  $\kappa = 0.5$  on the opposite side gives the best possible initial state tag. On the same side, the best sensitivity to mixing is obtained using  $\kappa = 1.0$ . In most events, the two hemispheres will have opposite charges, and  $-Q_{jo} Q_{js}$  will be positive. In events where a single mix has taken place the product of the charges will be smaller or negative.

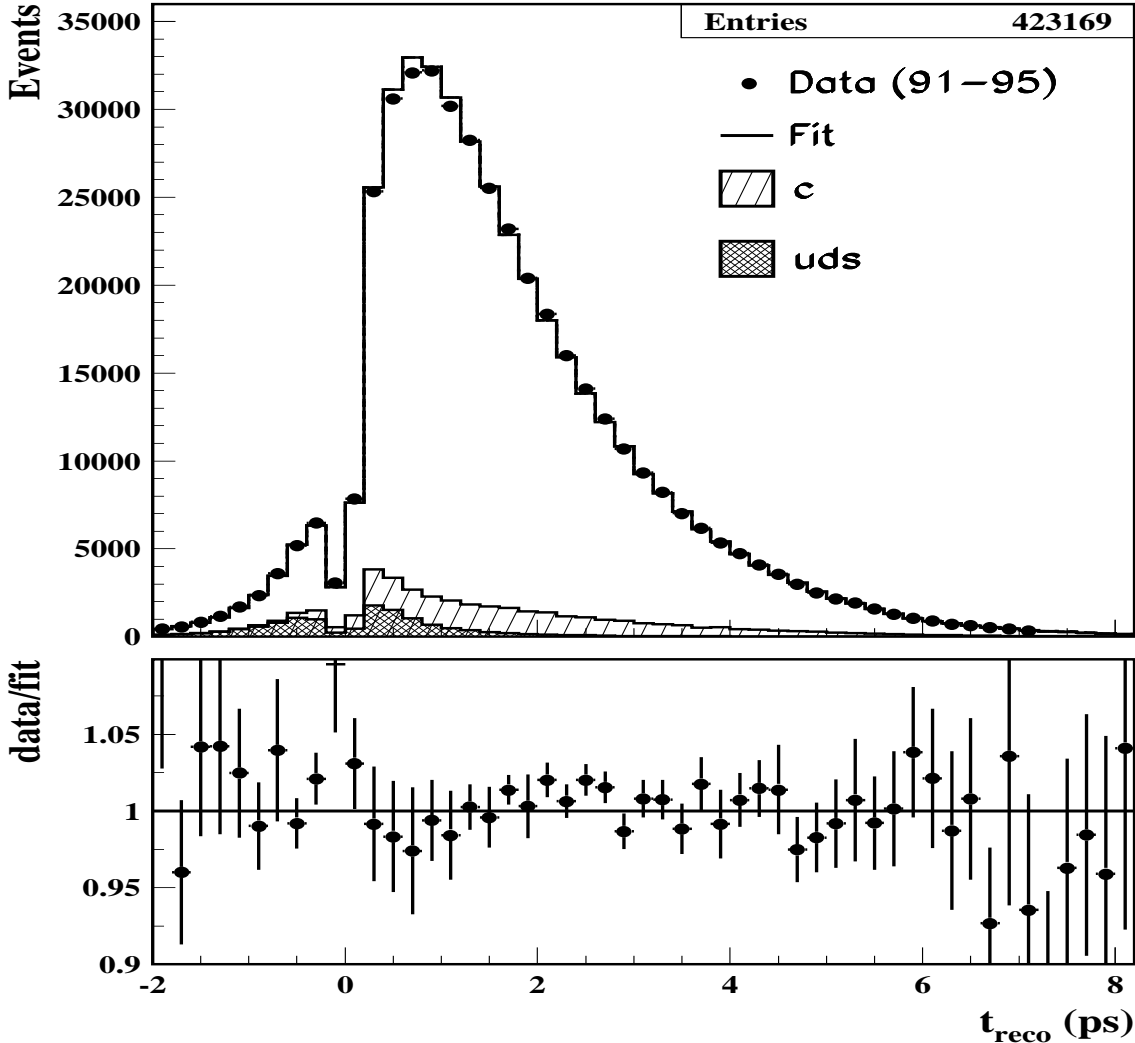


Figure 1: *Reconstructed proper time distribution in data and the result of the fit. Systematic errors from the  $b$  tagging efficiency are not included to highlight the observed discrepancy. The bottom plot shows the ratio of the measured distribution to the fit. The errors shown on the bottom plot include both the statistical errors from data and Monte Carlo and errors from the  $b$  tagging efficiency corrections.*

The charge correlation function contains mixing information from both sides of the event. On the same side there is direct dependence on  $\Delta m_d$  and  $\Delta m_s$  while on the side with no measured time there is dependence on the time integrated mixing parameters. In this analysis the charge correlation function is fitted for mixing on the same side only.

## 8.2 Jet-Charge Proper-Time and Multiplicity Corrections

A fit to the proper time dependence of the jet-charges in opposite hemispheres must take into account any possible bias induced by the algorithms used for vertexing and  $B$  momentum reconstruction. If this is not performed correctly then, even in the absence of a time-dependent mixing signal, there would be a variation of the charge correlation with reconstructed proper time.

The mean value of the jet-charge is delicate and sensitive to relatively small changes in the hemisphere multiplicity and longitudinal momentum distribution. On examination, the jet-charges of the various  $b$  hadron classes in Monte Carlo simulation do indeed exhibit a large and complex dependence on the reconstructed proper time. The cause of this is that the vertexing and revertexing algorithms are strongly dependent on the hemisphere track

multiplicity. This is because hemispheres with large numbers of tracks are more likely to be those where a primary track is accidentally included in the the secondary vertex calculation. This has the effect of “pulling” the secondary vertex closer to the primary, and hence forcing the event to appear at low proper times. This effect is clearly observed where the mean multiplicity at low reconstructed proper times is seen to be nearly  $\approx 25\%$  larger than the average.

Hence, it is possible to correct the proper time dependence of the jet-charges of each  $b$  hadron class based on the assumption that it is only the algorithmic effect of the vertexing which induces the observed shifts. The correction is applied using the observed multiplicity dependence for each  $b$  hadron class combined with the variation in the quark signed hemisphere charge for that class.

The observed discrepancies in the variation of the multiplicity with proper time between data and Monte Carlo simulation are passed through as errors on the jet-charge variation for each  $b$  hadron class. Hence, this degree of agreement is used to estimate the overall uncertainty applied to individual  $b$  hadron jet-charges in the  $\Delta m_d$  fit.

## 9 Fitting Procedure for $B_d^0 - \overline{B}_d^0$ Mixing

The fitting procedure to extract  $\Delta m_d$  is a multiparameter  $\chi^2$  minimisation consisting of two parts :

- A fit to  $\langle -Q_{jo}^{1.0} Q_{js}^{1.0} \rangle$  and  $\langle -Q_{jo}^{0.5} Q_{js}^{0.5} \rangle$  as a function of the BTAG cut in order to extract the values of  $\langle Q_b \rangle$ ,  $\langle Q_c \rangle$  and  $\langle Q_{uds} \rangle$  for  $\kappa = 0.5$  and  $\kappa = 1.0$ . This constrains the systematic uncertainties arising from the knowledge of these average jet charges.
- A fit to charge correlation function ,  $\langle -Q_{jo}^{0.5} Q_{js}^{1.0} \rangle (t)$ , as a function of reconstructed proper time to extract the value of  $\Delta m_d$ .

These are done simultaneously in a global fit which is explained in more detail below.

### 9.1 Fit for average jet charges

The value of  $\langle -Q_{jo}^\kappa Q_{js}^\kappa \rangle$  changes as a function of the BTAG cut which is applied because of the varying flavour composition and also because the BTAG algorithm alters the value of the jet-charges. The value of  $\langle -Q_{jo}^\kappa Q_{js}^\kappa \rangle$  after a BTAG cut in bin  $i$  can be written as :

$$\langle -Q_{jo} Q_{js} \rangle (i) = \mathcal{P}_b(i) \langle -Q_{jo} Q_{js} \rangle_b (i) + \mathcal{P}_c(i) \langle -Q_{jo} Q_{js} \rangle_c (i) + \mathcal{P}_{uds}(i) \langle -Q_{jo} Q_{js} \rangle_{uds} (i) \quad (6)$$

The variation of  $\langle -Q_{jo} Q_{js} \rangle$  for each flavour is due to the effect of the BTAG cut. These Monte Carlo distributions are used to calculate a bin dependent correction for each flavour, relative to the first bin (which is filled before the vertexing algorithm and any BTAG cut are applied). Equation (6) can then be written as :

$$\begin{aligned} \langle -Q_{jo} Q_{js} \rangle (i) &= \mathcal{P}_b(i) [ \langle -Q_{jo} Q_{js} \rangle_b (1) + \text{corr}_b(i) ] + \\ &\mathcal{P}_c(i) [ \langle -Q_{jo} Q_{js} \rangle_c (1) + \text{corr}_c(i) ] + \\ &\mathcal{P}_{uds}(i) [ \langle -Q_{jo} Q_{js} \rangle_{uds} (1) + \text{corr}_{uds}(i) ] \end{aligned} \quad (7)$$

where  $\text{corr}_f$  are the bin dependent corrections. In the first BTAG bin the hemispheres of the event are equivalent since no vertexing or tagging has been done and so :

$$\langle -Q_{jo} Q_{js} \rangle_f (1) = \langle Q_f \rangle^2 + \text{cov}(Q_{fo}, Q_{fs}) \quad (8)$$

where  $\text{cov}(Q_{fo}, Q_{fs})$  is the covariance between the hemisphere jet-charges for flavour  $f$  and is taken from the Monte Carlo. Hence by fitting the data distributions of  $\langle -Q_{jo}^{1.0} Q_{js}^{1.0} \rangle$  and  $\langle -Q_{jo}^{0.5} Q_{js}^{0.5} \rangle$  as a function of BTAG cut, it is possible to extract  $\langle Q_b \rangle$ ,  $\langle Q_c \rangle$  and  $\langle Q_{uds} \rangle$  for  $\kappa = 0.5$  and  $\kappa = 1.0$ .

The bin dependent purities are taken from the Monte Carlo and their errors are propagated through to the final result. The statistical correlations between the various BTAG bins are taken into account in the fit, as are the correlations (approximately 80%) between  $\langle -Q_{jo}^{1.0} Q_{js}^{1.0} \rangle (i)$  and  $\langle -Q_{jo}^{0.5} Q_{js}^{0.5} \rangle (i)$ . These correlations are measured from the data.

### 9.2 Fitting for $\Delta m_d$

The fit to the charge correlation as a function of reconstructed proper time is done in a similar way to the lifetime fit. In this case however, we consider the various classes of  $b$  hadron separately. The four *types* of  $b$  hadron (ie.

baryon,  $B^\pm$ ,  $B_d$ ,  $B_s$ ) are subdivided into six  $b$ -hadron *classes*, each of which has a different contribution to the charge correlation function.

The charge correlation in a reconstructed time bin  $j$  is given by a weighted sum of contributions from the various  $b$  classes and from backgrounds :

$$\langle -Q_{j_0}^{0.5} Q_{j_s}^{1.0} \rangle (j) = \frac{\mathcal{P}_b \sum_{class} f_{type} F_j^{class} \langle -QQ \rangle_j^{class} + \mathcal{P}_c F_j^c \langle -QQ \rangle_j^c + \mathcal{P}_{uds} F_j^{uds} \langle -QQ \rangle_j^{uds}}{\mathcal{P}_b F_j^b + \mathcal{P}_c F_j^c + \mathcal{P}_{uds} F_j^{uds}} \quad (9)$$

where  $F_j^{class}$  is the fraction of events in a given reconstructed proper time bin, as described in the lifetime fit. with the modification that the true theory  $T_i$  now involves the mixing dependence for the relevant classes<sup>2</sup>. The fraction  $f_{type}$  refers to  $f_\Lambda$ ,  $f_u$ ,  $f_d$  or  $f_s$ . Separate  $\mathbf{R}_{ij}$  matrices and efficiency corrections are used for the four different  $b$  types to take into account differences due to the different decay modes. Since the decay modes of  $B_s$  mesons are poorly known the effect of setting  $\mathbf{R}_{ij}(B_s) = \mathbf{R}_{ij}(B_d)$  is taken into account in the systematic error. The charge contribution from each class can be written as :

$$\langle -QQ \rangle_j^{class} = [\langle Q_b^{0.5} \rangle + corr_{Q_{b\text{BTAG}}}] [\langle Q_{class}^{1.0} \rangle + corr_{mult}(j)] + \text{correlation term} \quad (10)$$

The value of  $\langle Q_b^{0.5} \rangle$  is allowed to vary in the fit and is also constrained by the  $\langle -Q_{j_0} Q_{j_s} \rangle$  versus BTAG distributions. The correction to the average  $b$  jet-charge,  $corr_{Q_{b\text{BTAG}}}$ , is applied to account for the effect of the BTAG cut that is being used.  $\langle Q_{class}^{1.0} \rangle$  is the average jet-charge for this  $b$  class and  $corr_{mult}^{class}(j)$  is the bin dependent correction which must be applied to account for the multiplicity effects described in Section 8.2. The values of  $\langle Q_{class}^{1.0} \rangle$  are allowed to vary in the fit about a central Monte Carlo value within Gaussian constraints given in table 3. An additional constraint is imposed requiring that the weighted sum of the  $b$  class jet-charges is consistent with the average  $b$  jet-charge on the ‘same’ side ( $\kappa = 1.0$ ) :

$$\begin{aligned} \langle Q_b \rangle \pm 3\% &= f_u \langle Q_{B^\pm} \rangle + f_\Lambda \langle Q_\Lambda \rangle + \\ & f_d (1 - \chi_d) \langle Q_{B_{d_{unnmix}}} \rangle + f_d \chi_d \langle Q_{B_{d_{mix}}} \rangle + \\ & f_s (1 - \chi_s) \langle Q_{B_{s_{unnmix}}} \rangle + f_s \chi_s \langle Q_{B_{s_{mix}}} \rangle \end{aligned} \quad (11)$$

The charge correlation contributions from  $c$  and  $uds$  can be similarly expressed in terms of  $\langle Q_c^{0.5} \rangle$ ,  $\langle Q_c^{1.0} \rangle$  etc and are hence also constrained by the  $\langle -Q_{j_0} Q_{j_s} \rangle$  versus BTAG distributions. In this way, the absolute values of all jet-charges are allowed to vary in the fit, taking only the algorithm dependent corrections and correlation terms from Monte Carlo.

The  $b$  hadron lifetimes are allowed to vary within Gaussian constraints around the world-average values given in Table 3 and requiring that the weighted average is consistent with the measurement of the inclusive  $b$  lifetime,  $\tau_b$ .

$$\tau_b (\pm \sigma_{\tau_b}) = f_d \tau_{B_d} + f_u \tau_{B^\pm} + f_s \tau_{B_s} + f_{\Lambda_b} \tau_{\Lambda_b} \quad (12)$$

The production fractions,  $f_u$  and  $f_d$ , are expressed in terms of the  $B_s$  fraction,  $f_s$ , and the baryon fraction  $f_{\Lambda_b}$  :

$$f_d = f_u = \frac{1}{2}(1 - f_s - f_{\Lambda_b}) \quad (13)$$

The fractions  $f_s$  and  $f_{\Lambda_b}$  are also allowed to vary within Gaussian constraints and are also constrained by equations (11) and (12).

In summary, the parameters in Table 3 are varied in the global fit within the constraints indicated and imposing the additional constraints described above.

## 10 Results for $\Delta m_d$ and Systematic Uncertainties

The results of the fitting procedure for  $\Delta m_d$  in the various data-taking periods of LEP 1 are consistent with each other and hence compatible with the final result including the full statistical and systematic uncertainties. The individual  $\chi^2$  probabilities are excellent indicating that discrepancies are controlled and systematic errors are conservatively estimated.

The preliminary  $\Delta m_d$  result from the fit to the combined LEP 1 data-set is :

$$\Delta m_d = 0.441 \pm 0.026 \text{ (stat.)} \pm 0.029 \text{ (syst.) } ps^{-1}$$

The shape of the time-dependent charge correlation function is shown in Figure 2. The result of the fit is shown as a solid line and the expected distribution for a no-mixing hypothesis is shown as a dotted line.

The fitted  $\langle -Q_{j_0}^\kappa Q_{j_s}^\kappa \rangle$  ( $\kappa = 0.5, 1.0$ ) versus BTAG average jet-charge results are given in Table 4. A summary of

<sup>2</sup>For example for mixed  $B_d$  mesons  $T_i = \int \frac{e^{-t/\tau_{B_d}} (1 - \cos \Delta m_d t)}{2\tau_{B_d}} dt$ .



Parameter	Constraint
$\Delta m_d$	free
$\langle Q_b^{0.5} \rangle, \langle Q_c^{0.5} \rangle, \langle Q_{uds}^{0.5} \rangle$	free
$\langle Q_b^{1.0} \rangle, \langle Q_c^{1.0} \rangle, \langle Q_{uds}^{1.0} \rangle$	free
$\tau_{B_d}$	$1.56 \pm 0.06 ps$
$\tau_{B_s}$	$1.61 \pm 0.1 ps$
$\tau_{\Lambda_b}$	$1.14 \pm 0.08 ps$
$\tau_{B^+}$	$1.62 \pm 0.06 ps$
$\tau_b$	$1.570 \pm 0.014 ps$
$f_{\Lambda_b}$	$0.101 \pm 0.031$
$f_s$	$0.109 \pm 0.013$
$\langle Q_{\Lambda_b} \rangle$	$0.03170 \pm 10\%$
$\langle Q_{B^+} \rangle$	$0.1506 \pm 2\%$
$\langle Q_{B_{dnomix}} \rangle$	$0.1195 \pm 2\%$
$\langle Q_{B_{dmix}} \rangle$	$-0.05765 \pm 2\%$
$\langle Q_{B_{snomix}} \rangle$	$0.06958 \pm 10\%$
$\langle Q_{B_{smix}} \rangle$	$0.00763 \pm 10\%$
$\mathcal{P}_b$	$(87.5 \pm 1.2)\%$
$\mathcal{P}_c$	$(9.8 \pm 1.8)\%$

Table 3: Parameters and constraints used in the  $\Delta m_d$  fit.

Parameter	Fitted Value
$\langle Q_b^{0.5} \rangle$	$0.0780 \pm 0.0008$
$\langle Q_c^{0.5} \rangle$	$0.082 \pm 0.004$
$\langle Q_{uds}^{0.5} \rangle$	$0.1147 \pm 0.0007$
$\langle Q_b^{1.0} \rangle$	$0.114 \pm 0.001$
$\langle Q_c^{1.0} \rangle$	$0.090 \pm 0.008$
$\langle Q_{uds}^{1.0} \rangle$	$0.160 \pm 0.001$

Table 4: Fitted values for the mean jet-charges.

the individual systematic error contributions is given in Table 5. The systematic error for each individual source was determined for the fitted parameters by allowing that parameter to vary with the other free parameters whilst fixing all others. It is clear from Table 5, that adding the individual systematic error contributions in quadrature ignores many of the inter-correlations between parameters and inputs of the fit. For example, the constraints on the mean  $b$  lifetime are correlated with those on the individual lifetimes and the same is also true for the measured sum and  $b$  hadron components of the jet-charges. Given the preliminary nature of the current measurement, the uncorrelated error is used. The various sources of systematic uncertainty may be separated into the following general categories :

- *Lifetimes* : The  $b$  hadron fractions and lifetimes are allowed to vary in the fit within the Gaussian constraints given in Table 3. The fit has also been performed using the current world-average value of  $\tau_b = 1.549 \pm 0.02 ps$  instead of the value obtained from the fit to the proper time distribution. This results in a shift of  $3 \times 10^{-5} ps^{-1}$  in the fitted value of  $\Delta m_d$  and is hence neglected.
- *Jet-charges* : The combined statistical and systematic error on the fitted total  $b$  jet-charge is used to constrain the sum of the individual  $b$  hadron components. Additional errors are ascribed to account for possible conspiracies between the less well-known  $b$  hadron classes such as  $B_s$  and baryon decays. In addition, the errors from the multiplicity correction to the jet-charges are passed through bin-by-bin in  $t_{reco}$ .
- *Flavour Composition* : The sample composition obtained from the fit to data for  $\tau_b$  is used together with its full statistical and systematic uncertainties.
- *$b$  fragmentation* : This is studied using two methods, namely : (a) switching between the  $B_d$  and  $B_s$  unfolding matrices to take into account the current lack of knowledge about  $B_s$  decays and (b) varying the effective

Parameter	Variation	Fitted Value	$\sigma_{sys} (ps^{-1})$
$\tau_{B_d}$	$1.56 \pm 0.06 ps$	$1.591 \pm 0.056 ps$	0.0045
$\tau_{B_s}$	$1.61 \pm 0.1 ps$	$1.609 \pm 0.10 ps$	0.0022
$\tau_{\Lambda_b}$	$1.14 \pm 0.08 ps$	$1.144 \pm 0.08 ps$	0.003
$\tau_{B^+}$	$1.62 \pm 0.06 ps$	$1.599 \pm 0.058 ps$	0.004
$\tau_b$	$1.570 \pm 0.014 ps$	$1.560 \pm 0.04 ps$	0.0003
$f_{\Lambda_b}$	$0.101 \pm 0.031$	$0.080 \pm 0.021$	0.012
$f_s$	$0.109 \pm 0.013$	$0.1055 \pm 0.013$	0.0093
$\langle Q_{\Lambda_b} \rangle$	$0.03170 \pm 10\%$	$0.03188 \pm 0.0032$	0.0025
$\langle Q_{B^+} \rangle$	$0.1506 \pm 2\%$	$0.1510 \pm 0.0029$	0.012
$\langle Q_{B_{d_{nomix}}} \rangle$	$0.1195 \pm 2\%$	$0.1199 \pm 0.0023$	0.0063
$\langle Q_{B_{d_{mix}}} \rangle$	$-0.05765 \pm 2\%$	$-0.05769 \pm 0.0011$	0.0015
$\langle Q_{B_{s_{nomix}}} \rangle$	$0.06958 \pm 10\%$	$0.06992 \pm 0.0069$	0.004
$\langle Q_{B_{s_{mix}}} \rangle$	$0.00763 \pm 10\%$	$0.00763 \pm 0.0076$	0.0006
sample composition	$\mathcal{P}_b = (87.5 \pm 1.2)\%$ $\mathcal{P}_c = (9.8 \pm 1.8)\%$	$(87.4 \pm 1.1)\%$ $(8.9 \pm 1.2)\%$	0.004
$\Delta m_s$	$\infty \rightarrow 6 ps^{-1}$		+0.0001
set $\mathbf{R}_{ij}(B_s) = \mathbf{R}_{ij}(B_d)$			-0.0022
$\langle -QQ \rangle^{c,uds}$ time dependence	on/off		-0.005
$\epsilon_{BTAG}^b$ correction, $\mathcal{C}(j)$	on/off		+0.0002
multiplicity correction			0.008
peterson fragmentation	$\epsilon_b = 0.0045 \pm 0.0009$		0.015
MC statistics			0.001
Total			0.029

Table 5: Contributions to the systematic error on the  $\Delta m_d$  result. The upper part of the table corresponds to the fitted parameters and the second column gives the Gaussian constraints which are used. The third column gives the values returned from the fit. The lower part of the table corresponds to ‘fixed’ parameters. The fourth column gives the contribution of each source to the systematic error on  $\Delta m_d$ .

fragmentation function by reweighting the Monte Carlo, using the range of  $\epsilon_b$  values discussed in the lifetime fit.

- *Background jet-charges* : The effect of the corrections applied to the  $uds$  and  $c$  jet-charges to take into account their time-dependence is estimated by turning the time-dependence on and off in the fit and observing the effect on the value of  $\Delta m_d$ .
- $\Delta m_s$  : The effects of varying the input value of  $\Delta m_s$  between  $6 ps^{-1}$  and  $\infty$  is taken as an additional systematic error.

The dominant systematic uncertainties are currently due to the fractions of  $B_s$  mesons and baryons assumed in the sample and the average jet-charge for  $B^\pm$  mesons. The effects of varying the fragmentation function for  $b$  quarks are also seen to be significant.

## 11 Summary

A measurement of the average  $b$  lifetime using a fully inclusive vertexing method yields the value :

$$\tau_b = 1.601 \pm 0.004 (\text{stat.}) \pm 0.032 (\text{syst.}) ps$$

where the systematic error is currently dominated by uncertainties in the  $b$  fragmentation function. Using a double jet-charge technique, a time-dependent  $B_d$  mixing analysis gives :

$$\Delta m_d = 0.441 \pm 0.026 (\text{stat.}) \pm 0.029 (\text{syst.}) ps^{-1}$$

where the systematic error is currently dominated by a combination of the  $b$  fragmentation function uncertainty, the  $B_s$  and baryon fractions and possible conspiracies between the various  $b$  hadron jet-charges.

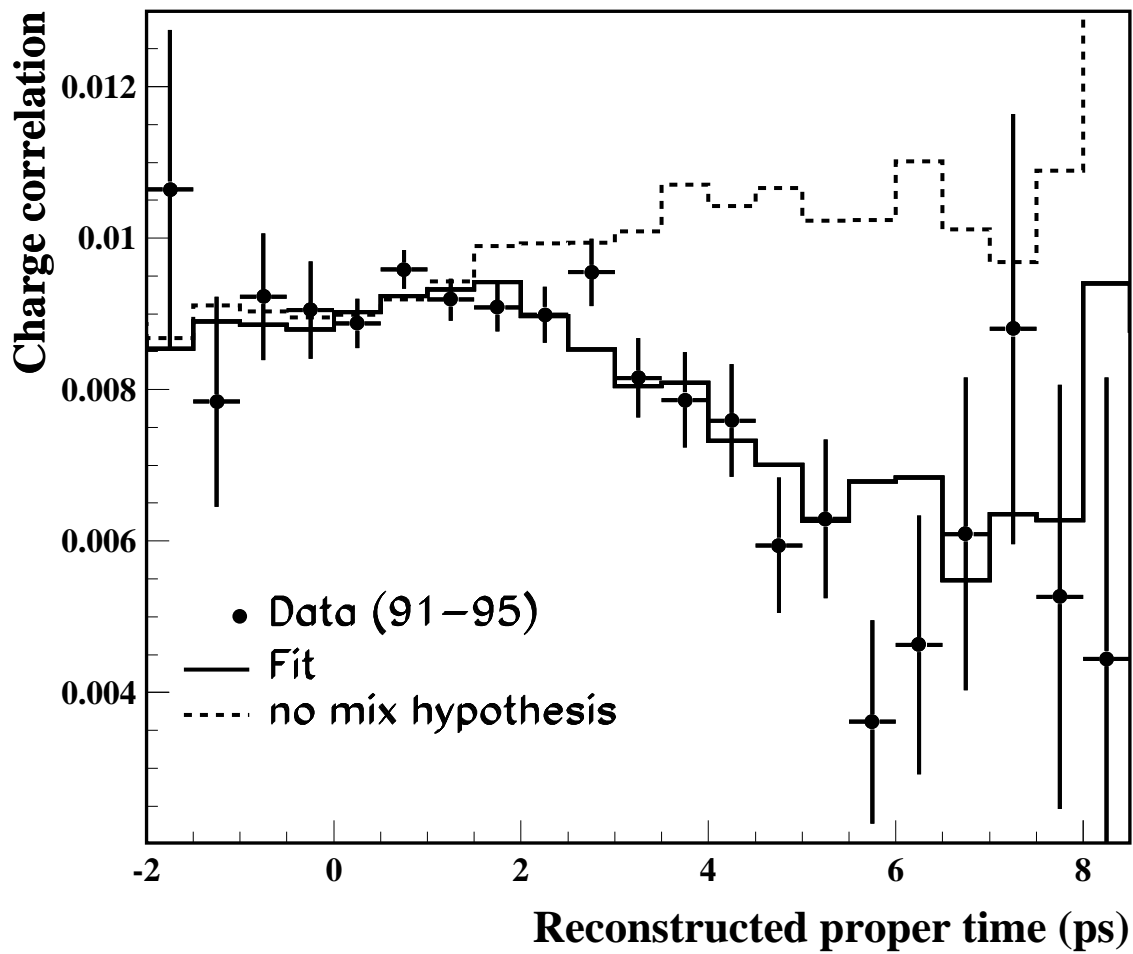


Figure 2: The charge correlation vs measured proper time with the result of the fit shown as the solid line. The no mixing hypothesis is shown as a dotted line.